control was robust and continued indefinitely without further adjustment.

The slight drift in frequency in Fig. 1B is attributable to a small and slow 100-Hz ramp in the injection current from the TDL control module. This drift shows that OPF control can be maintained while varying the center frequency of the TDL. We achieved similar results with a fixed Fabry-Perot etalon as the F/A by tuning the TDL to one side of a low-finesse etalon fringe. We maintained OPF control while scanning the frequency over a range of ~80 MHz. This range is of practical importance as it demonstrates that OPF can be used with a TDL to scan across a molecular absorption feature and to perform spectroscopic measurements at higher frequency resolution than previously possible.

We can only give an upper limit to the frequency stability attained with the OPF method because the measurements are dominated by detector noise that can only be improved by signal processing (Fig. 1). Another factor is that our F/A process inseparably convolves amplitude and frequency variations. To calculate an upper limit, we project the trajectories in two dimensions (Fig. 4A). A histogram of the number of points in each 0.2-MHz bin of the controlled and uncontrolled emission is then made (Fig. 4B). From a Gaussian fit to the controlled distribution, we obtain a value for its full width at half maximum (FWHM), here being 1.68 MHz, which we can use as a strict upper limit.

An equal partitioning of the intensity and frequency variations in quadrature, a reasonable assumption, would reduce the frequency limit by $\sqrt{2}$, to 1.19 MHz. The FWHM of the uncontrolled TDL excursion, measured by hand, is ~18 MHz. Therefore, the OPF method improves the TDL frequency stability by at least a factor of 11 to 15. We can determine more accurately the frequency stability by heterodyning the TDL output with a stabilized 10-μm CO_2 laser.

The improved stability, in both the frequency and the amplitude of the OPF-controlled TDL, will enable new applications. We have mentioned higher resolution spectroscopy that scans a TDL. An OPF-controlled TDL can also be used as a local oscillator for heterodyne radiometers. The far-infrared (FIR) spectral regime is extremely important, and the recent development of wide-bandwidth hot-electron bolometer mixers makes the need for a suitable FIR local oscillator immediate. There are numerous candidates for future OPF control, such as an optically pumped submillimeter laser that emits from 30 μm to 1 mm and whose output varies in a seemingly random fashion because of nonlinear feedback between the pump and lasant gas.

REFERENCES AND NOTES

1. "Chaos in Communications," *Proc. SPIE 2038* (1993).
2. E. Ott, C. Grebogi, J. A. Yorke, *Phys. Rev. Lett.* **64**, 1196 (1990).
3. U. Dressler and G. Nitsche, *ibid.* **68**, 1 (1992); F. Romeiras, C. Grebogi, E. Ott, W. P. Dayawansa, *Physica D* **58**, 165 (1992); H. Wang and E. H. Abed, *Proceedings of IFAC Nonlinear Control Systems Symposium*, Bordeaux (1992).
4. W. L. Ditto, S. N. Rauseo, M. L. Spano, *Phys. Rev. Lett.* **65**, 3211 (1990).
5. J. Singer, Y.-Z. Wang, H. H. Bau, *ibid.* **66**, 1123 (1991).
6. A. Garfinkel, M. L. Spano, W. L. Ditto, J. N. Weiss, *Science* **257**, 1230 (1992).
7. E. R. Hunt, *Phys. Rev. Lett.* **67**, 1953 (1991).
8. T. Takizawa, Y. Liu, J. Ohtsubo, *IEEE J. Quantum Electron.* **30**, 334 (1994).
9. R. Roy, T. W. Murphy Jr., T. D. Maier, Z. Gills, E. R. Hunt, *Phys. Rev. Lett.* **68**, 1259 (1992); Z. Gills, C. Iwata, R. Roy, I. B. Schwartz, I. Triandaf, *ibid.* **69**, 3169 (1992).
10. D. E. Jennings, *J. Quant. Spectrosc. Radiat. Transfer* **40**, 221 (1988).
11. ———, *Appl. Opt.* **23**, 1299 (1984).
12. J. P. Eckmann and D. Ruelle, *Rev. Mod. Phys.* **57**, 617 (1985).
13. J. P. Eckmann, S. O. Kamphorst, D. Ruelle, S. Ciliberto, *Phys. Rev. A* **34**, 4971 (1986).
14. M. Ding, C. Grebogi, E. Ott, T. Sauer, J. A. Yorke, *Phys. Rev. Lett.* **70**, 3872 (1993).
15. D. S. Broomhead and G. P. King, *Physica D* **20**, 217 (1986).
16. N. H. Packard, J. P. Crutchfield, J. D. Farmer, R. S. Shaw, *Phys. Rev. Lett.* **45**, 712 (1980).
17. An animated phase portrait of one of our data sets can be viewed on our World Wide Web site at http://aurora.phys.utk.edu/~senesac/
18. T. W. Carr and I. B. Schwartz, *Phys. Rev. E* **51**, 5109 (1995); *Physica D*, in press.

19. We thank J. Lobell for designing the OPF electronics and G. Miller for putting it together [they are in Code 692 of the Goddard Space Flight Center (GSFC)]. M. Sirota and D. Reuter (Code 693) loaned us the diode laser for this experiment. This research was conducted under NASA cooperative agreement NCC 5-88 with the University of Tennessee under the support of the GSFC Director's Discretionary Fund.

29 July 1996; accepted 23 September 1996

Solar Wind Magnetic Field Bending of Jovian Dust Trajectories

H. A. Zook,* E. Grün, M. Baguhl, D. P. Hamilton, G. Linkert, J.-C. Liou, R. Forsyth, J. L. Phillips

From September 1991 to October 1992, the cosmic dust detector on the Ulysses spacecraft recorded 11 short bursts, or streams, of dust. These dust grains emanated from the jovian system, and their trajectories were strongly affected by solar wind magnetic field forces. Analyses of the on-board measurements of these fields, and of stream approach directions, show that stream-associated dust grain masses are of the order of 10^{-18} gram and dust grain velocities exceed 200 kilometers per second. These masses and velocities are, respectively, about 10^3 times less massive and 5 to 10 times faster than earlier reported.

While the Ulysses spacecraft was in the neighborhood of Jupiter, the on-board cosmic dust detector (CDD) detected 11 intense, and unexpected, streams of dust (*1–3*). The first stream occurred 2359 Jupiter radii (R_J, where 1 R_J = 71,398 km) from Jupiter, and 137 days before Ulysses' closest approach to Jupiter (JCA) on 8 February 1992. The last stream occurred at a distance of 4205 R_J, or about 2 astronomical units (AU), from Jupiter and 254 days after JCA. The dust grains in these streams are believed to have come from the jovian system (*2*) for two reasons: (i) the most intense stream, of 327 impacts onto the CDD, occurred only 31 days after JCA, and 327 R_J from Jupiter; (ii) stream radiants tended to lie on, or near, the line of sight (LOS) direction to Jupiter from the CDD. Both phenomena are shown in Fig. 1, where dust stream impacts are characterized by being unusually concentrated in the measured spacecraft rotation angle, ϕ_m, and in time (*4*). Each stream appears to impact the CDD from a single direction unique to that stream. The variation in ϕ_m is largely due to the 140° field-of-view (fov) of the CDD as it rotates through a stream radiant, although a few degrees of variation in ϕ_m may be due to a true spread in arrival directions of the dust grains. Strong non-gravitational forces must be acting on the grains during their trajectories from Jupiter because, under gravitational forces alone, average stream radiants would lie within a degree or two of the LOS direction to Jupiter. This was only true for streams S5 and S6. Analysis of CDD data from the Galileo spacecraft, which recorded even more intense streams of jovian dust than Ulysses (*5*), suggested that Jupiter's moon, Io, is a likely source of the dust (*6*).

H. A. Zook and J.-C. Liou, SN3, NASA Johnson Space Center, Houston, TX 77058, USA.
E. Grün, M. Baguhl, G. Linkert, Max-Planck-Institut für Kernphysik, Postfach 103980, 69029 Heidelberg, Germany.
D. P. Hamilton, Department of Astronomy, University of Maryland, College Park, MD 20742–2421, USA.
R. Forsyth, The Blackett Laboratory, Imperial College, London SW7 2BZ, UK.
J. L. Phillips, Los Alamos National Laboratory, Los Alamos, NM 87545, USA.

*To whom correspondence should be addressed. E-mail: zook@snmail.jsc.nasa.gov

Here we will focus on whether the reported impacting dust grain masses and velocities (10^{-15}g $\leq m \leq 4 \times 10^{-14}$ g and 20 km/s $\leq V_{imp} \leq$ 56 km/s) (*2*, *3*) are compatible with the observed direction of approach of the streams to Ulysses. If they are not compatible, we determine what size particles, traveling at what velocity, and charged to what electrostatic potential are responsible for the observed streams (*7*).

The CDD detects dust by measuring the charge of the impact plasma created by an impact of a particle onto the CDD surface. To estimate the size, velocity, and charge of these particles, we numerically simulate the ejection at the median time of each stream occurrence, backward in time and outward away from Ulysses, of a large number (typically 10^7) of electrically charged dust particles. Particles are ejected in all directions that can be sensed during spacecraft rotation, and are ejected with many sizes and velocities. The equations of motion, assuming acceleration due to gravitational and solar wind magnetic field forces on each ejected grain, are then numerically integrated backward in time (reversing also the directions of the solar wind magnetic field vector, and the particle, spacecraft, and solar wind velocity vectors), to see if the grain approaches to within 50 R_J of Jupiter. If it does, we consider it a potential solution in the sense that the same particle could have left the jovian magnetosphere, traveled forward in time through the time-variable solar wind magnetic field, and impacted the CDD. If, in addition, the dust grain's simulated ϕ lies within the 95% confidence limits of the average ϕ_m, it is considered a realistic solution for that stream. It is numerically efficient to integrate backward in time, because the integration starts at a known location and time (the spacecraft location at the mean time of stream impact), as well as at known solar wind velocity and magnetic field intensity values.

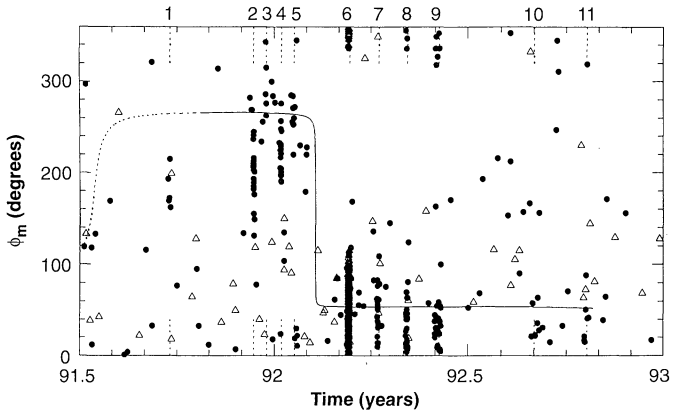

Fig. 1. Dust particle impacts on the Ulysses CDD versus measured spacecraft rotation angle, ϕ_m, and time. Solid circles correspond to 1.16×10^{-14}C $\leq Q <$ 4.46×10^{-14}C and open triangles correspond to 4.46×10^{-14}C $\leq Q <$ 1.73×10^{-13}C, where Q is the amplitude of the total positive ion charge extracted from the impact plasma (*14*, *15*). Dust streams, indicated by vertical dashed lines, are labeled 1 through 11, and are recognized when dust impacts are concentrated in time and rotation angle (*16*). The solid line indicates when the CDD axis points closest to Jupiter, and Jupiter is in the fov of the CDD. The sudden change in rotation angle on 8 February 1992 occurred as Ulysses flew by Jupiter. In the dashed portion of the line, Jupiter never entered the CDD fov.

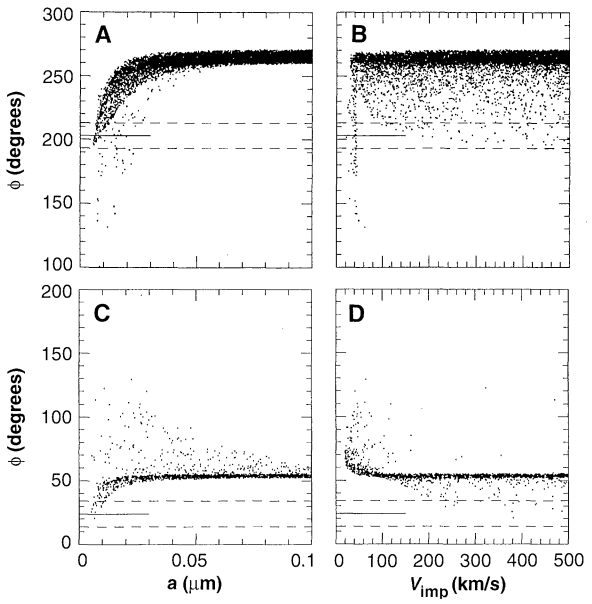

Fig. 2. (**A**) Calculated spacecraft rotation angle, ϕ, versus particle radius, a, for the 7798 (of 10^7) time-reversed simulated trial trajectories of stream *S2* that passed within 50 R_J of Jupiter. The horizontal dashed lines 10° above and below the mean ϕ_m at 203° give the approximate 95% confidence limits on the true location of the mean ϕ_m. (**B**) ϕ versus V_{imp} for the same calculated trajectories. (**C**) ϕ versus a for the 1409 simulated trajectories (again of 10^7) of stream *S9* that passed within 50 R_J of Jupiter. (**D**) ϕ versus V_{imp} for the calculated trajectories of stream *S9*. The mean $\phi_m = 24°$ and 95% confidence limits are labeled as in (A).

The quantitative analysis is outlined below: For each grain simulated, a random number generator selects parameters a, V_{imp}, θ, and ϕ in each of the following ranges:

$$0\ \mu m < a \leq 0.1\ \mu m;$$
$$20\ km/s \leq V_{imp} \leq 500\ km/s;$$
$$15° \leq \theta \leq 155°;\ 0° \leq \phi < 360° \quad (1)$$

where a is particle radius, θ is the angle of dust grain emission relative to the spacecraft spin axis (which points toward the Earth), and ϕ is the emission direction around the Ulysses spin axis. As the solar wind velocity (*8*) and magnetic field (*9*) vectors are continuously measured on Ulysses, the total vector acceleration, $\mathbf{a}_p$, of a charged dust grain can be determined by

$$\mathbf{a}_p = -GM_S\mathbf{r}_S/r_S^3 - GM_J\mathbf{r}_J/r_J^3 + (Q/m)(\mathbf{v} \times \mathbf{B}) \quad (2)$$

where $\mathbf{r}_S$ is the position vector from the sun to the dust grain, $\mathbf{r}_J$ is the position vector from Jupiter to the dust grain, and $\mathbf{v} = \mathbf{v}_p - \mathbf{v}_{SW}$, where $\mathbf{v}_p$ and $\mathbf{v}_{SW}$ are, respectively, the dust grain and solar wind velocity vectors. G is the gravitational constant, M_S and M_J are the masses of the sun and Jupiter, respectively, and $\mathbf{B}$ is the solar wind magnetic field vector. $\mathbf{B}$ ranged from 0.2 to 5 nT from 60 days before *S1* to the day that the last stream, *S11*, was recorded and averaged about 1 nT. $\mathbf{v}_{SW}$ ranged from about 400 to 600 km/s, and averaged about 450 km/s during the same period. The initial time-reversed $\mathbf{v}_p$ is related to impact velocity, V_{imp}, the impact velocity of the dust grain on the CDD, by $\mathbf{v}_p = -(V_{imp} - \mathbf{v}_{SC})$ where $\mathbf{v}_{SC}$ is the spacecraft velocity. The charge, Q, on a dust grain is due to a balance between solar photo-electron emission and neutralization by solar wind electrons. The resulting dust grain electric potential, V, is somewhat uncertain, but +5 V is near the average Ulysses spacecraft potential inferred from the solar wind electron spectrum, and is used here. The dust grain charge-to-mass ratio, Q/m, is given by

$$Q/m \sim V/(\rho a^2) \quad (3)$$

The dust grain mass density, ρ, is assumed to be 1 g/cm^3. All quantities are transformed to ecliptic cartesian coordinates, an inertial system for the numerical integration. Considering only the x-components of acceleration, velocity, and position, the $(i + 1)$th iteration values of v_{px} and x_p are related to the ith iteration values by

$$v_{px}(i + 1) = v_{px}(i) + a_{px}(i)\Delta t_p(i) \quad (4)$$

$$x_p(i + 1) = x_p(i) + v_{px}(i)\Delta t_p(i) + 0.5a_{px}(i)[\Delta t_p(i)]^2 \quad (5)$$

where $a_{px}(i)$ is obtained from Eq. 2, $v_{px}(i)$ and $x_p(i)$ are the velocity and position of the dust grain at the beginning of the ith interval, and $\Delta t_p(i)$ is defined below. $x_p(0)$ and $v_{px}(0) = -(V_{impx} - v_{SCx})$ are the particle position and velocity at the time of impact, respectively. The y and z components are treated in an identical fashion.

Care must be used in the evaluation of $\Delta t_p(i)$. For each ith-interval, 1-hour averages are taken of the Ulysses-measured vector components of the solar wind velocity and magnetic field, and $\Delta t_p(i)$ is the length of time the particle spends in the corresponding ith interval. Except for an assumed weakening of the magnetic field vector components with increasing distance from the sun (*10*), it is assumed that all vectors remain unchanged in direction as they are carried radially outward at the measured solar wind velocity. If, for example, the particle is traveling, forward in time toward the sun at radial velocity component, $v_{pR}(i)$, then, approximately, it travels through the ith interval in a time (in hours) of $\Delta t_p(i) = v_{SW}(i)/[v_{pR}(i) + v_{SW}(i)]$. Other smaller corrections to $\Delta t_p(i)$ are required due to spacecraft motion, dust grain acceleration, and due to the assumption that the solar wind velocity and magnetic field vectors rotate with the sun. Magnetic field and solar wind velocity vectors are assumed, as an approximation, not to vary with solar latitude out to −12° latitude.

For particles that were simulated to impact on the CDD at the median time of occurrence of stream S2 (Fig. 2A) only particles with radii in the range $0.006\ \mu m < a < 0.026\ \mu m$ have ϕ's that lie within the 95% confidence bars of the measured mean ϕ_m (derived from data in Fig. 1). Larger particles arrive from close to the LOS direction to Jupiter; the width in ϕ for larger particles is due to the 100 R_J width of the jovian magnetosphere as seen from Ulysses. A subgroup of particles with $V_{imp} < 45$ km/s (Fig. 2B) gives rise to a group (Fig. 2A) whose particle radii lie between 0.014 and 0.023 μm. However, detailed laboratory calibrations with iron, carbon, and silicate particles impacting on a CDD with $V_{imp} < 50$ km/s showed (*11*) that the resulting impact plasmas for particles less than 0.026 μm in radius would be expected to be at least one order of magnitude below the detection threshold of 10^{-14} C. If particles below the experimental detection threshold are eliminated from our numerical results, then only particles with $0.006\ \mu m < a < 0.014\ \mu m$ (Fig. 2A), lie within the acceptable confidence interval and only velocities greater than about 100 km/s are acceptable (Fig. 2B). A particle trajectory, representing one point from Fig. 2, A and B, is shown in Fig. 3.

For stream S9, only particle trajectories with radii in the range $0.005 < a < 0.01$ μm and $V_{imp} > 200$ km/s are compatible with the mean ϕ_m for that stream (Fig. 2, C and D). These simulations also show that particles with radii less than 0.005 μm are unable to make the journey from Jupiter to Ulysses; all these particles, for every stream, are caught up in the solar wind and swept away (a particle of radius 0.01 μm traveling at 450 km/s across a 1 nT magnetic field feels a solar wind $\mathbf{v} \times \mathbf{B}$ force 2500 times greater than the force of solar gravity at 5 AU). It appears that the particles in every stream except S6 have similar sizes and impact velocities; the S6 impact plasmas are somewhat larger than for the other streams.

The use of the solar wind magnetic field as a giant mass-and-velocity spectrometer for charged dust grains has constrained dust grain radii and velocities suggesting that they are small and fast. Our results are consistent with the model of Horanyi *et al.* (*12*), who have shown that the jovian magnetosphere can accelerate dust grains, of the sizes that we modelled, to velocities in excess of 300 km/s. We agree with Hamilton and Burns (*13*) that the temporal variation of the interplanetary magnetic field (IMF) primarily determines changes in the directionality of dust grains impacting on the CDD on board Ulysses. But our modeling uses the measured, rather than their postulated, solar wind magnetic field; from this, we find the particles to be much smaller than the ones they modeled.

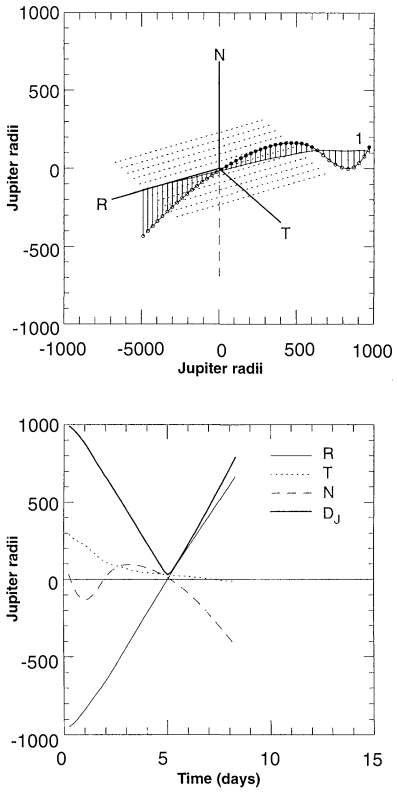

Fig. 3. The calculated trajectory of a dust grain in stream *S2*, whose time-reversed trajectory passed within 50 R_J of Jupiter. The dust grain was of density 1 g/cm^3, of radius 0.0069 μm, and impacted the CDD at a velocity of 316 km/s. It arrived from a ϕ of 201.8°, and from a θ of 95.7°. The flight time to Jupiter was 5.04 days and the distance of closest approach to Jupiter was 29.7 R_J. (**Top**) The trajectory in three dimensions in a coordinate system centered on Jupiter. The **R** direction is positive to the left and outward from the sun along the sun-Jupiter line. The **T** direction is perpendicular to **R** and is parallel to the ecliptic plane, and **N** = **R** × **T** points close to ecliptic north. The trajectory starts at the label 1 at the right-center of the diagram and proceeds, in reverse-time, radially outward from the spacecraft to Jupiter. The part of the trajectory to the left of Jupiter does not represent physical reality for particles originating in the jovian system. Solid dots and open circles indicate that the trajectory is, respectively, above or below, the **R**-**T** plane. (**Bottom**) The **R**, **T**, and **N** components of the above trajectory, as well as the total distance, D_J, from Jupiter versus reversed time.

The use of the solar wind magnetic field as a giant mass-and-velocity spectrometer for charged dust grains has constrained dust grain radii and velocities suggesting that they are small and fast. Our results are consistent with the model of Horanyi *et al.* (*12*), who have shown that the jovian magnetosphere can accelerate dust grains, of the sizes that we modelled, to velocities in excess of 300 km/s. We agree with Hamilton and Burns (*13*) that the temporal variation of the interplanetary magnetic field (IMF) primarily determines changes in the directionality of dust grains impacting on the CDD on board Ulysses. But our modeling uses the measured, rather than their postulated, solar wind magnetic field; from this, we find the particles to be much smaller than the ones they modeled.

REFERENCES AND NOTES

1. E. Grün *et al.*, *Science* **257**, 1550 (1992) described their observation of the first stream.
2. E. Grün *et al.*, *Nature* **262**, 428 (1993) described six streams and suggested a jovian source for these streams.
3. M. Baguhl *et al.*, *Planet. Space Sci.* **41**, 1085 (1994) found 5 additional streams in the Ulysses' CDD dataset.
4. $\phi_m = 0$ when the CDD axis points as close as possible to ecliptic north. Events of digital amplitude higher than 8 are left out of Fig. 1 as they are largely due to impacts by interstellar grains (*2*, *3*) and nearly all occur between streams. This omission highlights the stream data. With 15 impacts in a stream, and considering the 140° fov of the CDD, the true radiant of a monodirectional stream is known, at 95% confidence, to ±10°. The spacecraft spin axis is coaligned with the high gain antenna, which points toward the Earth. The central axis of the 140° fov CDD is fixed to point at 85° to the Ulysses spin axis.
5. E. Grün *et al.*, *Nature* **381**, 395 (1996).
6. E. Grün *et al.*, *Science* **274**, 399 (1996).
7. A brief description of stream *S8* is given in H. A. Zook *et al.*, Proceedings of the *150th Colloquium of the International Astronomical Union*, Gainesville, FL, 14–18 August 1995, B. S. Gustafson and M. S. Hanner, Eds. (Astronomical Society of the Pacific, San Francisco, 1996), vol. 104, p. 23.
8. S. J. Bame *et al.*, *Geophys. Res. Lett.* **20**, 2323 (1993).
9. A. Balogh *et al.*, *ibid.*, p. 2331.
10. F. Mariani and F. M. Neubauer, in *Physics of the Inner Heliosphere*, R. Schwenn and E. Marsch, Eds., (Springer-Verlag, New York, 1990), pp. 99–181.
11. J. R. Göller and E. Grün, *Planet. Space Sci.* **37**, 1197 (1989).
12. M. Horanyi, G. Morfill, E. Grün, *Nature* **363**, 144 (1993).
13. D. P. Hamilton and J. A. Burns, *ibid.* **364**, 695 (1993).
14. E. Grün *et al.*, *Planet. Space Sci.* **43**, 941 (1995).
15. E. Grün *et al.*, *ibid.*, p. 971.
16. Only streams *S2* and *S9* are analyzed here. Of the 23 impacts in stream *S2*, 19 occurred within an 8-hour period; their associated mean ϕ_m was 203°. The median time of occurrence of this stream was 58 days before JCA and at a distance of 997 R_J. Stream *S9* consisted of 33 particles that impacted over a period of 5.85 days, occurred 116 days after JCA and 1968 R_J (0.939 AU) from Jupiter. The mean ϕ_m for this stream was 24°.

17. We appreciate review comments by M. Cintala, B. Gustafson, and an anonymous reviewer.

25 July 1996; accepted 22 October 1996